Reexamination of the evolution of the dynamic susceptibility of the glass former glycerol

S. Adichtchev, T. Blochowicz, C. Tschirwitz, V. N. Novikov, and E. A. Rössler*
Experimentalphysik II, Universität Bayreuth, D 95440 Bayreuth, Germany
(Received 30 September 2002; published 14 July 2003)

The dielectric data of glycerol compiled by Lunkenheimer *et al.* [Contemp. Phys. **41**, 15 (2000)] are reanalyzed within a phenomenological approach on the one hand, and within mode coupling theory (MCT), on the other. We present a complete interpolation of the dielectric data covering 17 decades in frequencies. The crossover temperature extracted from the phenomenological analysis of the slow response at low temperatures and defined by the emergence of the excess wing upon cooling agrees well with the critical temperature extracted from a MCT analysis of the dynamics at high temperatures including data that were not used in the first MCT analysis of glycerol by Lunkenheimer *et al.* [Phys. Rev. Lett. **77**, 318 (1996)]. The crossover temperature is found to be $T_c = 288 \pm 3$ K, which is significantly higher than previously reported. Extracting the nonergodicity parameter f, the characteristic anomaly is only found when $1-f$ is inspected, since f is very close to 1. No difference for the evolution of the dynamic susceptibility is observed for the nonfragile system glycerol with respect to fragile glass formers provided that the evolution of the dynamics is studied as a function of the correlation time τ_α.

DOI: 10.1103/PhysRevE.68.011504 PACS number(s): 64.70.Pf, 78.35.+c, 61.43.Fs

I. INTRODUCTION

In recent years significant experimental progress has been made in monitoring the evolution of the molecular dynamics in supercooled liquids. For example, the dielectric response of polar glass formers can now be measured over 18 decades in frequency (10^{-5}–10^{13} Hz) [1]. Quasielastic light scattering is able to monitor the fast dynamics with high precision (10^{8}–10^{13} Hz) [2–5] and neutron scattering experiments have compiled the corresponding q dependence [6,7]. Together with molecular dynamics simulations [8], the applications of the aforementioned techniques among others have demonstrated that mode coupling theory (MCT) [9,10] provides a rather consistent description of the evolution of the susceptibility at the onset of the glass transition, i.e., at high temperatures. In addition to the main α-process, a fast relaxation process is identified, leading to a two-step decay of the correlation function. Within MCT the fast process is attributed to some in-cage motion whereas the α-process describes the reorganization of the cage which enables flow. A MCT analysis allows for determining a critical temperature T_c above which the high temperature scenario of the (idealized) theory well accounts for the salient features of the susceptibility [10].

Most systems investigated so far were fragile molecular glass formers, characterized by the absence of strong intermolecular interactions. Here, the question arises whether MCT may also apply to nonfragile glass formers, i.e., to so-called strong systems with more or less strong intermolecular interactions. Since in such systems the cage effect is expected to play a minor role, one may be reluctant to test MCT here. However, it turns out that again two-step correlation functions are observed though quantitative agreement with MCT is less convincing [11–13]. The case of glycerol is of particular interest since it is an organic system of intermediate degree of fragility. Several MCT studies were published, but concerning the critical temperature T_c extracted from the data significant disagreement was found. In 1994 the first MCT analysis of light scattering (LS) as well as of neutron scattering (NS) data was carried out by Wuttke *et al.* [14] and the authors reported $T_c \cong 225$ K, however, no agreement with viscosity data was obtained. The latter data suppose $T_c \cong 300$ K as pointed out by Rössler *et al.* [15]. A reanalysis of the LS data by Franosch *et al.* [16] identified T_c in the temperature interval 223–233 K, but the result was not fully compelling. In 1996 an analysis of the now accessible high frequency dielectric (DS) data of glycerol were presented by Lunkenheimer *et al.* [17] and they reported $T_c \cong 262$ K. In a review paper on testing MCT predictions by NS, Petry and Wuttke [6] displayed the nonergodicity parameter for several glass formers though they hesitated to draw any conclusion in the case of glycerol. However, reinspecting their plot $T_c \cong 280$ K may be suggested. Finally, an impulsive stimulated thermal scattering study by Paolucci and Nelson [18] "rule(s) out the possibility of a marked anomaly in the temperature region from 228 to 268 K."

Clearly, these disparate results are very unsatisfying and they may point to a problem for any MCT analysis, namely, that the theory's expected range of validity is not well defined. In other words, the approximations made within the theory are not controlled. On the one hand, the theoretical predictions are expected to hold only close to the critical temperature T_c, on the other, for temperature close to T_c the high temperature scenario of MCT is expected to be disturbed by the emergence of the so-called hopping transport, which within the extended theory is supposed to provide the mechanism to reestablish ergodicity below T_c. It is expected that this problem is more severe in nonfragile glass formers than in fragile systems. Experimentally, the situation turns out to be somewhat different. In a series of papers it was demonstrated that the high temperature scenario of MCT is found to hold even up to the fluid regime close to T_m [7,8,19]. In turn this provides a large enough temperature

*Author to whom correspondence should be addressed. Email address: ernst.roessler@uni-bayreuth.de

range from which the critical temperature can be accurately determined via extrapolation and allows one to easily identify first deviations from the scaling laws indicating the breakdown of the (idealized) MCT description at $T \leqslant T_c$. Most of the cited analyses of glycerol were carried out in a rather small temperature range which actually may be too small. As a consequence, it may happen that the results of these analyses depend on the temperature interval investigated.

Below the dynamic crossover at T_c, the evolution of the susceptibility is not adequately described by the theory and one has to resort to phenomenological approaches. Analyzing the dielectric loss of several glass formers including glycerol by applying a distribution of correlation times derived from an extension of a generalized gamma distribution first introduced by Kudlik *et al.* [20], Blochowicz *et al.* [21] report that, independent of the degree of fragility, the evolution of the dynamic susceptibility including the α-relaxation peak together with its high frequency excess wing exhibits a high degree of universality provided that the parameters of the excess wing are plotted as a function of the correlation time τ_α rather than as a function of temperature as is usually done. Within this analysis it can be shown that the excess wing appears first at $\log_{10}(\tau_\alpha/s) \cong -8$ upon cooling and that the temperature at which this happens correlates well with the critical temperature T_c of MCT. This phenomenological analysis provides clear evidence that a high and low temperature scenario holds for the evolution of the susceptibility, and it was concluded that the breakdown of the high temperature scenario of MCT coincides with the appearance of the excess wing. For glycerol $T(\log_{10} \tau_\alpha = -8) \cong 270$ K is found, thus challenging most MCT analyses on glycerol published so far. Although the nature of the excess wing is not well understood, it seems to be some kind of a secondary relaxation process and cannot be identified with a contribution from hopping transport [22,23].

In this contribution we reanalyze the dielectric data compiled by Lunkenheimer *et al.* [1] (cf. Fig. 1), which currently provide the most complete dielectric dataset reported for a glass former. By applying the extension of the gamma distribution [20,21] for describing the slow response at low temperatures on the one hand, and analyzing the dynamics at high temperatures as proposed by MCT, on the other, we will demonstrate that (i) a complete interpolation of the dielectric data covering about 17 decades in frequencies is obtained and (ii) the crossover temperature extracted from the phenomenological analysis agrees well with that obtained from the MCT analysis. For the purpose of the latter analysis we included high temperature data [1] that were not used in the first MCT analysis of the dielectric response [17]. In this work, Lunkenheimer *et al.* analyzed directly the $\varepsilon(\omega)$ data whereas we use normalized data for which the static permittivity has been scaled out. Since glycerol is a nonfragile glass former, the effect of the temperature dependence of the static susceptibility is quite strong and significantly changes the results of any line-shape analysis. (iii) Finally, we will show that no difference is found for the nonfragile glass former glycerol with respect to a fragile glass former, e.g., propylene carbonate.

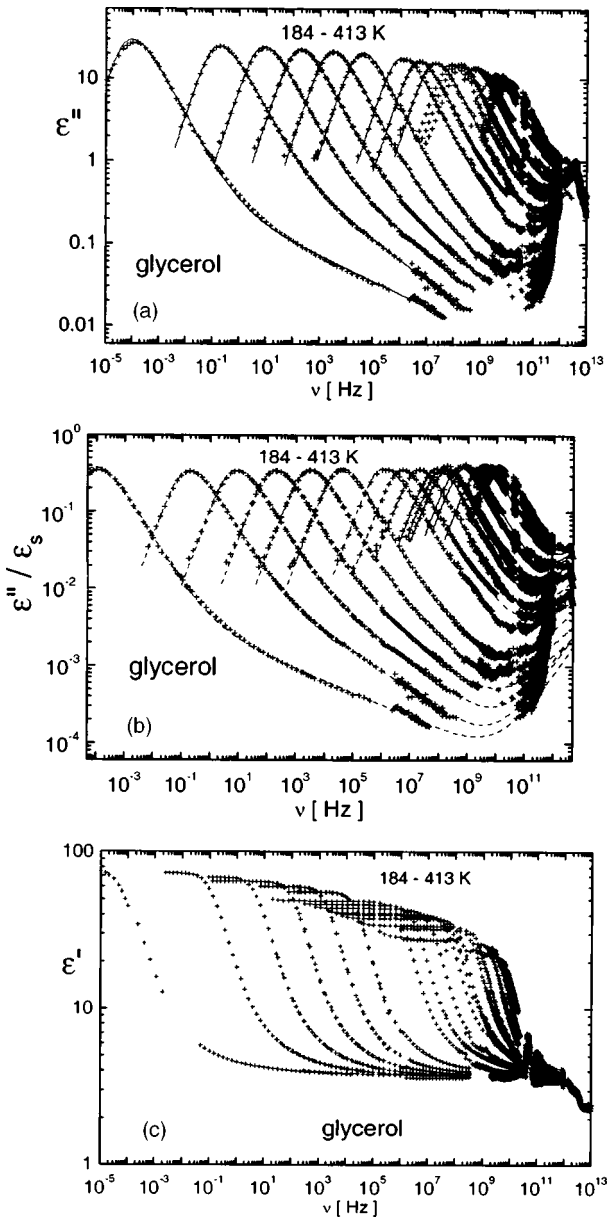

FIG. 1. Dielectric permittivity of glycerol as compiled by Lunkenheimer *et al.* [1] for various temperatures. The temperature of each curve is, from left to right (in kelvin), 184, 195, 204, 213, 223, 234, 253, 263, 273, 289, 295, 303, 323, 333, 363, 382, 403, and 413. (a) Imaginary part $\varepsilon''(\nu)$, included fit (solid line) by applying the GGE distribution of correlation times, Eq. (5), for interpolating the slow response ($\nu < 1$ GHz) at $T \leqslant 273$ K. (b) Imaginary part scaled by the static permittivity ε_s, included is complete interpolation of the relaxational contribution by applying Eq. (10) (dashed line) and by applying in addition the constraint, Eq. (9) (solid line), data for highest temperatures not fitted, cf. Fig. 5. (c) Real part $\varepsilon'(\nu)$ as compiled by Lunkenheimer *et al.* [1], no data for 403 K; note double logarithmic scale.

II. THEORETICAL BACKGROUND

A. MCT predictions

We first summarize the asymptotic scaling predictions of the idealized MCT [9,10]. Due to the interplay of fast dy-

namics and α-process a minimum is found in the susceptibility in the gigahertz regime, which at $T>T_c$ is interpolated by

$$\chi''=\chi''_{\min}[b_{\mathrm{MCT}}(\nu/\nu_{\min})^{a_{\mathrm{MCT}}} + a_{\mathrm{MCT}}(\nu/\nu_{\min})^{-b_{\mathrm{MCT}}}]/(a_{\mathrm{MCT}}+b_{\mathrm{MCT}}), \quad (1)$$

where $\nu_{\min}$ and $\chi''_{\min}$ are the frequency and the amplitude of the minimum. The exponents a_{MCT} and b_{MCT} determine the low-frequency behavior of the fast dynamics and the high-frequency part of the α-process, respectively. They are determined by a single parameter, namely, the exponent parameter λ, thus are not independent. The temperature dependence of $\nu_{\min}$, $\chi''_{\min}$, and the time scale τ_α are expected to be given by

$$\chi''_{\min}\propto\varepsilon^{1/2}, \quad \nu_{\min}\propto\varepsilon^{1/2a_{\mathrm{MCT}}}, \quad \tau_\alpha\propto\varepsilon^{-\gamma_{\mathrm{MCT}}}, \quad T>T_c \quad (2)$$

with $\varepsilon=T-T_c$. The exponent γ_{MCT} is related to the exponents a_{MCT} and b_{MCT} via $\gamma_{\mathrm{MCT}}=1/(2a)+1/(2b)$.

From $\chi''_{\min}(T)$, $\nu_{\min}(T)$, and $\tau_\alpha(T)$ the critical temperature T_c should follow; the latter terminates the temperature interval of the high temperature scenario of MCT. Below T_c the fast relaxation spectrum is expected to change its shape. A crossover from a power law with an exponent a_{MCT} at high frequencies to a white noise spectrum ($a=1$) at low frequencies is expected. As a consequence of the appearance of this ''knee'' a decrease of the fast dynamics relaxation strength is forecast upon cooling. This constitutes the anomaly of the nonergodicity parameter f, a generalized Debye-Waller factor, which defines the relaxation strength of the slow dynamics (α-process). A characteristic temperature dependence is predicted

$$f(T)=f_c, \quad T>T_c; \quad f(T)=f_c+h\delta^{1/2} \quad T<T_c, \quad (3)$$

where h is some constant and $\delta=T_c-T$. Here, for the analysis of the DS data, the q dependence of f has been dropped. Above T_c the parameter f remains temperature independent, whereas below T_c it quickly rises. We note that the knee has not been observed so far in molecular glass formers and the clear identification of the anomaly of the nonergodicity parameter is a matter of debate [24]. It has been suggested [4,5] that it may appear advantageous to actually determine the quantity $1-f$ which presents the fraction that decays due to processes faster than the α-process and is given by the integral over the susceptibility of the fast relaxation $\chi''_{fast}(\nu)$,

$$1-f\propto\int_{-\infty}^{\infty}\chi''_{\mathrm{fast}}(\nu)d\ln\nu\cong\int_{\nu\gg1/\tau_\alpha}^{\infty}\chi''(\nu)d\ln\nu. \quad (4)$$

B. Phenomenological description of the susceptibility

Glycerol is a type-*A* glass former exhibiting no discernible secondary relaxation peak in the dielectric spectra. For such systems Kudlik *et al.* [20] (for details, see also Blochowicz *et al.* [21]) have proposed a distribution of correlation times which excellently interpolates the α-relaxation contribution including both peak and excess wing. The distribution is an extension of a generalized gamma distribution (GGE) [25] and is given by

$$G_{\mathrm{GGE}}(\ln\tau)=N_{\mathrm{GGE}}(\alpha,\beta,\gamma)\exp\left[-\frac{\beta}{\alpha}\left(\frac{\tau}{\tau_0}\right)^{\alpha}\right]\left(\frac{\tau}{\tau_0}\right)^{\beta}\times\left[1+\left(\frac{\tau\sigma}{\tau_0}\right)^{\gamma-\beta}\right] \quad (5)$$

with the normalizing factor

$$N_{\mathrm{GGE}}(\alpha,\beta,\gamma)=\alpha\left(\frac{\beta}{\alpha}\right)^{\beta/\alpha}\left[\Gamma\left(\frac{\beta}{\alpha}\right)+\sigma^{\gamma-\beta}\left(\frac{\alpha}{\beta}\right)^{(\gamma-\beta)/\alpha}\Gamma\left(\frac{\gamma}{\alpha}\right)\right]^{-1} \quad (6)$$

given by the condition $\int_{-\infty}^{\infty}G_{\mathrm{GGE}}(\ln\tau)d\ln\tau=1$.

The mean time constant reads

$$\langle\tau\rangle=\tau_0\left(\frac{\alpha}{\beta}\right)^{1/\alpha}\frac{\Gamma\left(\frac{\beta+1}{\alpha}\right)+\sigma^{\gamma-\beta}\left(\frac{\alpha}{\beta}\right)^{(\gamma-\beta)/\alpha}\Gamma\left(\frac{\gamma+1}{\alpha}\right)}{\Gamma\left(\frac{\beta}{\alpha}\right)+\sigma^{\gamma-\beta}\left(\frac{\alpha}{\beta}\right)^{(\gamma-\beta)/\alpha}\Gamma\left(\frac{\gamma}{\alpha}\right)}. \quad (7)$$

In addition to parameters α and β specifying the manifestation of the α-relaxation peak, two additional parameters σ and γ appear, which define the onset of the wing and its exponent, respectively. Thus, in this phenomenological approach it is assumed that the wing contribution formally may be treated as a part of the α-relaxation spectrum. We emphasize that the width parameters α and β can assume values $0<\alpha$, $\beta<\infty$, and γ is not to be confused with γ_{MCT}.

In the Appendix we further discuss the role of the two parameters α and β, which in the GGE distribution are needed to model the α relaxation around the maximum. In short, β controls the widths of the relaxation peak, whereas α fixes details of the peak, in particular, at low frequencies $\nu<\nu_{\max}$. It turns out [21] that for a given glass former, α can be kept constant for all temperatures while β changes with temperature in a characteristic way (see below).

From Eq. (5) the complex dielectric permittivity $\varepsilon(\omega)$ is calculated as

$$\varepsilon_\alpha(\omega)-\varepsilon_\infty=\Delta\varepsilon_\alpha\int_{-\infty}^{\infty}G_{\mathrm{GGE}}(\ln\tau)\frac{1}{1+i\omega\tau}d\ln\tau, \quad (8)$$

where $\Delta\varepsilon_\alpha$ is the relaxation strength of the α-process.

As demonstrated by Adichtchev *et al.* [5] and by Blochowicz *et al.* [21], in the case of glycerol, 2-picoline, and propylene carbonate the parameters σ and γ evolve in a very similar manner provided that they are plotted as a function of τ_α (cf. also Fig. 4). Moreover, it has been shown that the excess contribution appears only at $\tau_\alpha>10^{-8}$ s and that at high temperatures the susceptibility is well described by a

Cole Davidson (CD) function [26], i.e., by a simple peak function. It turns out that the GGE distribution provides an excellent fit of a CD susceptibility with $\gamma=\beta_{\mathrm{CD}}$, when a constraint $\sigma(\alpha,\beta,\gamma)=\sigma_c$ is introduced in such a way that the absolute short time asymptote of the GGE and the CD distribution become identical. Explicitly, one finds [21]

$$\sigma_c(\alpha,\beta,\gamma) = \left(\frac{\left(\frac{\beta}{\alpha}\right)^{\beta/\alpha}\left(\frac{\alpha\pi}{\sin(\pi\gamma)}-\left(\frac{\alpha}{\beta}\right)^{\gamma/\alpha}\Gamma(\gamma/\alpha)\right)}{\Gamma(\beta/\alpha)} \right)^{1/(\beta-\gamma)}. \quad (9)$$

Irrespective of the particular shape of the α peak itself, the constraint σ_c assures that no wing is present in $\varepsilon''(\omega)$. Thus, although the distribution function GGE at $\tau/\tau_0 \ll 1$ is still described by two power-law contributions with exponents β and γ, the resulting susceptibility function is a simple peak function being very close to a CD susceptibility. Note that a fit of a CD susceptibility by the GGE distribution always leads to $\gamma=\beta_{\mathrm{CD}}$, hence applying the constraint only one parameter, namely, β has to be optimized. Qualitatively, for the typical values of the parameters α and β found in the type-*A* systems, the onset parameter σ reaches values of 1–2, i.e., the onset of the excess wing shifts very close to the peak frequency $1/(2\pi\tau_\alpha)$ and as consequence the susceptibility becomes a simple peak function without an excess wing. Simultaneously, the parameter β becomes >1 [21]. Concluding, instead of a free fit of the data, the constraint, Eq. (9), can be applied to guarantee that the GGE is well reproducing a simple peak susceptibility. We shall call this limit the CD limit of the GGE distribution. As the line-shape analysis shows, beyond this limit (not applying the constraint) a pronounced excess wing is characterized by an onset parameter $\sigma \gg 1$ and a parameter $\beta<1$.

In order to account also for the fast dynamics we include in the phenomenological approach a power-law contribution, explicitly

$$\chi''(\nu)=A\chi''_{\mathrm{GGE}}(\nu)+B\nu^a. \quad (10)$$

The MCT scenario can easily be implemented in the phenomenological approach by assuming that $a=a_{\mathrm{MCT}}$ and $\gamma=b_{\mathrm{MCT}}$ holds in addition to applying the constraint Eq. (9). Within this approach the $1-f$ [cf. Eq. (4)] is defined by

$$1-f=\frac{B\int_{-\infty}^{\ln \nu_c}\nu^a d\ln\nu}{\pi A/2+B\int_{-\infty}^{\ln \nu_c}\nu^a \ln\nu}, \quad (11)$$

where for an experimental analysis the cutoff frequency ν_c has to be properly chosen. A and B are some weighting factors that may depend on temperature.

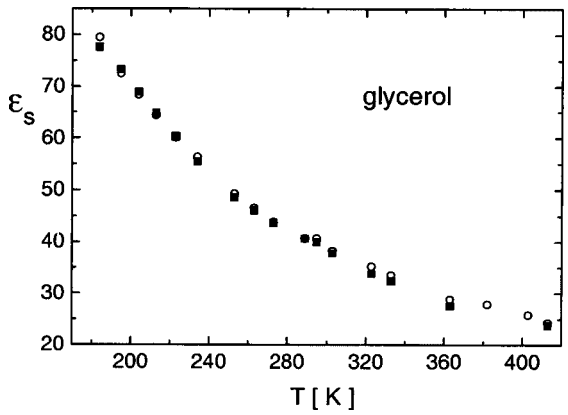

FIG. 2. Temperature dependence of the static permittivity ε_s (solid squares); for comparison the data reported by Lunkenheimer *et al.* [1] are shown (open circles).

III. RESULTS

A. Phenomenological analysis

Figure 1(a) presents the imaginary part $\varepsilon''(\nu)$ and Fig. 1(c) presents the real part $\varepsilon'(\nu)$ of glycerol as a function of frequency as compiled by Lunkenheimer *et al.* [1]. About 18 decades in frequency are covered. As is clearly seen from the data, the amplitude of the α-relaxation peak decreases with increasing temperature. This is a consequence of the temperature dependence of the static dielectric constant $\varepsilon_s=\Delta\varepsilon+\varepsilon_\infty$. The relaxation strength $\Delta\varepsilon$ includes all contributions from intermolecular dynamics, namely, that of the α-process and fast dynamics as well as that of the boson peak and the microscopic peak; ε_∞ comprises all process at optical frequencies. The quantity ε_s may be extracted from the plateau of $\varepsilon'(\nu)$ at lowest frequencies [cf. Fig. 1(c)]. Figure 2 displays the results. For comparison, the corresponding results reported by Lunkenheimer *et al.* [1] are included showing a good agreement. Inspecting the real part [cf. Fig. 1(c)] it is found that $\Delta\varepsilon \gg \varepsilon_\infty$ holds for all temperatures. Therefore, for obtaining a normalized susceptibility we take

$$\chi''(\nu)=\varepsilon''(\nu)/\varepsilon_s \quad (12)$$

and only this quantity can be compared against theory. Note that the static quantity ε_s contains no direct information on the dynamics. Thus, from analyzing its temperature dependence, no conclusion can be drawn in a strict sense concerning a dynamic crossover as may be is suggested by Lunkenheimer [27] and by Schönhals [28]. Figure 1(b) presents such scaled data. Within the experimental noise the α-relaxation peak is constant in amplitude essentially for all temperatures.

Starting with the line-shape analysis, in Fig. 1(a) we demonstrate that the slow response (<1 GHz) at low temperature ($T<289$ K) including the α-relaxation peak and excess wing is well described by the phenomenological approach, namely, by the GGE distribution, Eq. (5). The parameters of the fits are displayed as a function of temperature in Fig. 3. The onset parameter σ and the exponent γ [cf. Figs. 3(a) and 3(b)], both characterizing the excess wing, as well as the

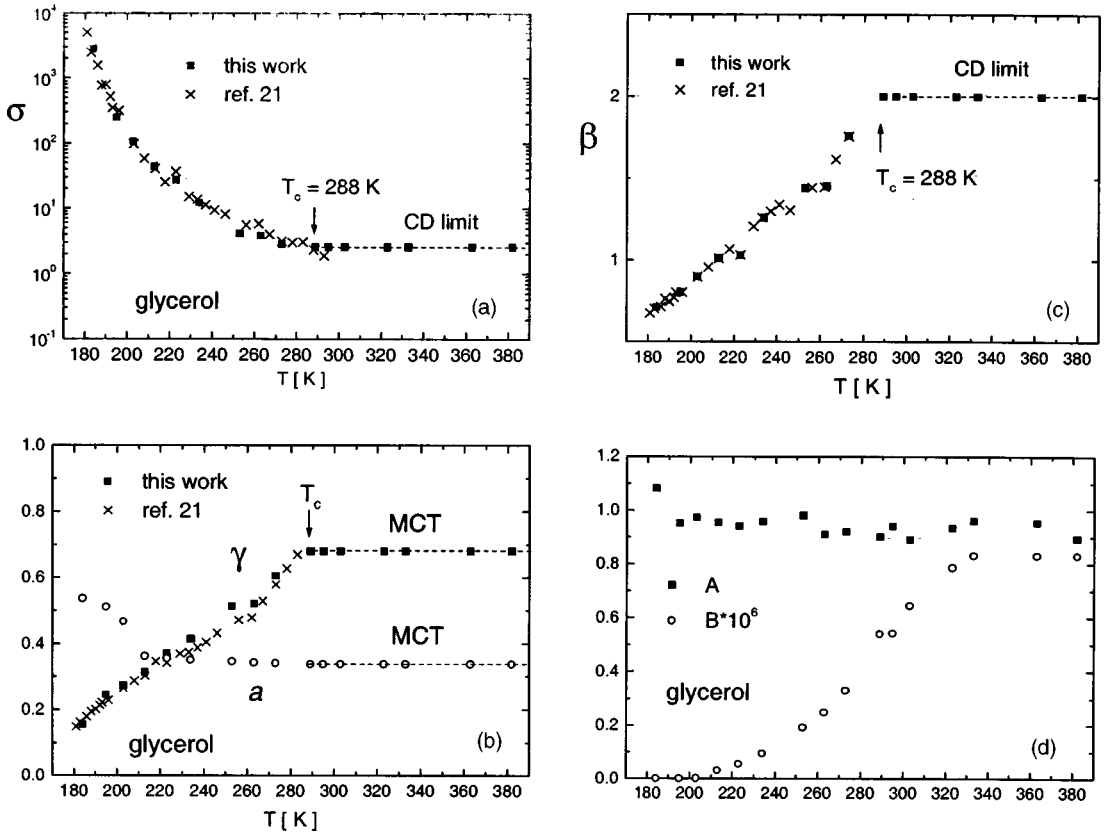

FIG. 3. Fit parameters of the GGE distribution as well as the parameters of the fast dynamics contribution obtained from interpolating the dielectric spectra of glycerol in Figs. 1(a), 1(b), and 5 as a function of temperature T. (a) Onset parameter σ of the excess wing; (b) exponent γ of the excess wing and exponent a of the fast dynamics contribution; (c) width parameter β; (d) amplitude of the α-process A and fast dynamics contribution B; at high temperatures the Cole-Davidson (CD), respectively, MCT limit is indicated.

parameter β [cf. Fig. 3(c)], determining together with α (which for glycerol can be set to $\alpha=10$ for all temperatures) the width of the α-relaxation peak, are found to be very similar to those reported by Blochowicz *et al.* [21] who performed an analysis of a dataset extending only up to 1 GHz. The exponent γ becomes lower, the lower the temperature and σ strongly increases with decreasing temperature. This means that the excess wing becomes more and more pronounced upon cooling, in the sense that it gets flatter and the wing onset is shifted to higher frequencies with respect to the α peak. Parameter β shows a trend to increase with temperature, in particular, it becomes larger than 1 at the highest temperatures. Blochowicz *et al.* [21] also reported the GGE parameters of the glass formers propylene carbonate and 2-picoline, which may be compared to those of glycerol if the parameters are plotted as a function of $\log_{10}\tau_\alpha$. This is done in Fig. 4. Although the degree of fragility is quite different within this group of materials, a very similar behavior is found for σ and γ, and also for β at low temperatures. In first approximation $\log_{10}\sigma$ linearly increases with $\log_{10}\tau_\alpha$, i.e., with the state of supercooling, whereas γ nonlinearly decreases reaching values of about 0.15 at highest $\log_{10}\tau_\alpha$, that is, at lowest temperatures. The actual difference among the three glass formers present in the spectra is reflected only by the width parameter α, which may be set to a temperature independent value for each glass former. Its value can reliably be found from fitting the spectra complied around T_g. We find $\alpha=10$, 20, 5 for glycerol, propylene carbonate, and picoline, respectively.

Since at high temperatures the exponent γ strongly increases, σ becomes close to 1 and β becomes larger than 1 [cf. Fig. 3(c)], a clear indication is given that the CD limit is reached (cf. Sec. II B). In other words, at $T>289$ K or $\tau_\alpha < 2\,10^{-9}$ the excess wing has disappeared, and one finds $\beta_{\mathrm{CD}}=\gamma$ when a CD function is chosen to interpolate the high temperature susceptibility. Therefore, we apply for higher temperatures ($T>289$ K) the GGE distribution together with the constraint, Eq. (9), which, as discussed, provides an interpolation of a simple peak susceptibility, which is very close to a CD function. The result of this fitting procedure is shown in Fig. 5 where we display the normalized high temperature data of glycerol. Here, we included a power-law contribution with a temperature independent exponent $a=0.337$ (cf. the MCT analysis below) in order to account properly for the fast dynamics contribution up to, say, 200 GHz. It turns out that the data are compatible with keeping $\gamma=0.68$ ($=\beta_{\mathrm{CD}}$) as well as β independent of temperature (cf. Fig. 3). Clearly, also this phenomenological fit yields a satisfying interpolation of the data demonstrating that above 289 K the different subspectra are virtually not changing in

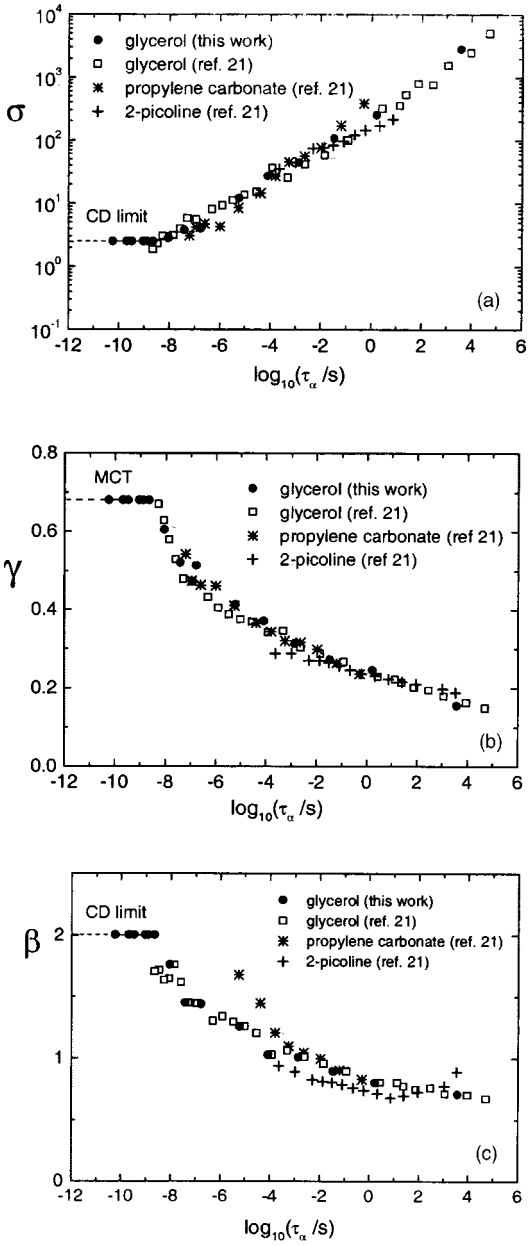

FIG. 4. Fit parameters of the susceptibility of the α-process as a function of $\log_{10}\tau_\alpha$; included are the corresponding data for glycerol, propylene carbonate, and 2-picoline taken from Ref. [21]; the Cole-Davidson (CD), respectively, MCT limits are indicated. (a) Wing parameter σ; (b) wing exponent γ; (c) width parameter β.

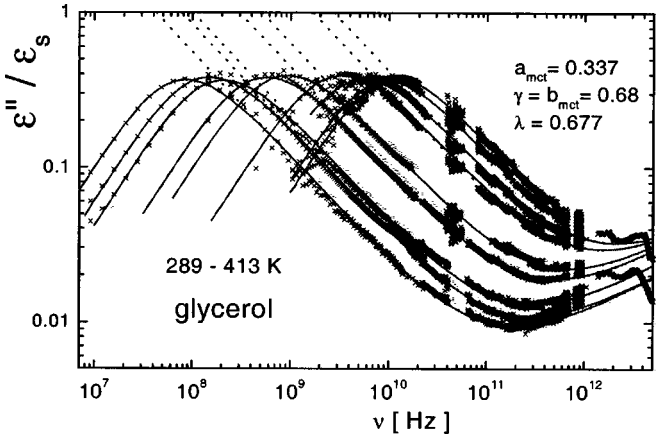

FIG. 5. Normalized imaginary part of the complex permittivity at high temperatures ($T=289$, 295, 303, 323, 333, 363, 382, 403, and 413 K); interpolation of both α-process and fast dynamics contribution by the GGE distribution with applying the constraint, Eq. (10), and $\gamma=0.68$ (solid lines) together with a power-law contribution with $a=0.337$ accounting for the fast dynamics contribution. For comparison MCT interpolation of the minimum with $b_{\mathrm{MCT}}=0.68$ and $a_{\mathrm{MCT}}=0.337$ (dashed lines) is shown at 403 and 413 K a fit by a Cole-Davidson susceptibility is shown.

shape any longer. Here, we want to note that the data are characterized by very different point densities in the frequency intervals covered by different techniques. Also, the scatter is quite large at high frequencies. Therefore, the fits show small systematic deviations from the data in some cases, and our analysis can only demonstrate that the data are compatible with the MCT predictions.

In Fig. 1(b) fits of the full dataset are shown including the constrained fits above 289 K as well as those below by applying free fits with the GGE distribution together with a power-law contribution for the fast dynamics. Clearly a satisfying interpolation is obtained covering 17 decades in frequency. The temperature dependence of the GGE parameter, as well as the parameters of the fast dynamics contribution, i.e., the exponent a and the corresponding weighting factors A and B [cf. Eq. (10)], are included in Fig. 3. At high temperatures ($T>289$ K) the exponents γ and a are essentially temperature independent, whereas at low temperatures they show a marked temperature dependence. Exponent γ is found to be the same as that obtained from the sole analysis of the slow dynamics shown in Fig. 1(a), demonstrating that this exponent can be also reliably determined from the data without accounting for the fast dynamics contribution. Below 289 K, the exponent a of the fast dynamics contribution shows a trend to increase. The weighting factor A is virtually constant whereas B, reflecting the fast dynamics contribution, decreases strongly below about 320 K. Again, we note that the present dielectric data of glycerol do not allow for an unambiguous determination of the exponent a.

Regarding the evolution of the susceptibility the phenomenological approach provides clear evidence for a high temperature regime and a low temperature regime with a crossover temperature $T_x\cong 290$ K. Whereas at high temperatures $T>T_x$ a simple peak susceptibility with constant relaxation strength (reflected by $A\cong$const) describes the α-process together with a temperature independent fast dynamics contribution (reflected by $B\cong$const) with a constant exponent a, a new spectral feature appears at low temperatures ($T<290$ K), namely, the excess wing. In addition, the weight of the fast dynamics contribution becomes strongly temperature dependent [cf. parameter $B(T)$]. In Fig. 3 the two regimes are marked and, as we will demonstrate next, the high temperature scenario is also well described by mode coupling theory.

B. Mode coupling theory analysis

In the second approach we analyze the evolution of the susceptibility as described by the high temperature scenario of the MCT. The theory provides an interpolation of the minimum according to Eq. (1). Regarding this minimum, a sum of the constrained GGE susceptibility (or a CD function) and a power-law accounting for the fast dynamics is mathematically equivalent to Eq. (1) provided that $\gamma = b_{\mathrm{MCT}}$ and $a = a_{\mathrm{MCT}}$ are chosen. Actually, for the phenomenological fit shown in Fig. 5 we have already incorporated the MCT relation between γ and a derived from an exponent parameter $\lambda = 0.677$ [9]. Consequently, the phenomenological fit (solid line) and the MCT interpolation by Eq. (1) (dashed line) of the susceptibility minimum are indistinguishable as is demonstrated in Fig. 5. The phenomenological approach covers the complete relaxational spectra, whereas MCT provides a generic interpolation of the minimum, only. Thus, the high temperature regime is described within the phenomenological approach by exponents that are compatible with MCT.

Having obtained the minimum parameters χ''_{min} and ν_{min} by the MCT interpolation, one is able to test the scaling laws of MCT, Eq. (2). Figure 6 presents the results for the linearizing relationships $(\chi''_{\mathrm{min}})^2(T)$, $\nu_{\mathrm{min}}^{2a_{\mathrm{MCT}}}(T)$ and $\tau_\alpha^{-1/\gamma_{\mathrm{MCT}}}(T)$ as well as $\eta^{-1/\gamma_{\mathrm{MCT}}}(T)$ as functions of temperature [cf. Eq. (2)]. Here, τ_α is obtained from the phenomenological fit and the viscosity η is taken from the literature [29]. Consistently, a critical temperature $T_c \cong 288 \pm 3$ K can be extracted by extrapolating the high temperature data $\chi''_{\mathrm{min}}(T)$, $\nu_{\mathrm{min}}(T)$, and $\tau_\alpha(T)$, only. The viscosity data extrapolate to a somewhat higher value of T_c, a phenomenon indicating that η and τ_α may exhibit a slightly different temperature dependence at high temperatures. We emphasize that first deviations from the scaling laws appear at somewhat higher temperature than T_c. Once again we note that in the previous MCT analysis by Lunkenheimer *et al.* [17] the analysis was restricted to temperatures $T \leqslant 333$ K. Also, their parameter $b_{\mathrm{MCT}} = 0.63$ is somewhat different from that obtained within the present analysis ($b_{\mathrm{MCT}} = 0.68$). Only by including the high temperature data and a normalized susceptibility can a consistent critical temperature be extracted from all the observables, and, consequently, the critical temperature is found to be significantly higher with respect to the analysis of Lunkenheimer *et al.* reporting $T_c = 262$ K.

Another way of demonstrating the validity of the MCT predictions is to rescale the data $\chi''(\nu)$ by χ''_{min} and ν_{min} in such a way as to obtain a master curve for the susceptibility minimum. This is demonstrated in Fig. 7. Here we present the data above the critical temperature $T_c = 288$ K (solid points) as well as below (crosses). Clearly, all data above $T_c = 288$ K can be collapsed onto a master curve for the envelope which is well interpolated by the MCT formula with $b_{\mathrm{MCT}} = 0.68$ and $a_{\mathrm{MCT}} = 0.337$ as is also revealed by the minimum interpolation in Fig. 5, whereas below 288 K deviations show up, namely, the minimum becomes broader and broader, the lower the temperature. This feature reflects the appearance of the excess wing below T_c. In other words, the emergence of the excess wing terminates the high temperature scenario of MCT, and thus allows to identify unambiguously the critical temperature.

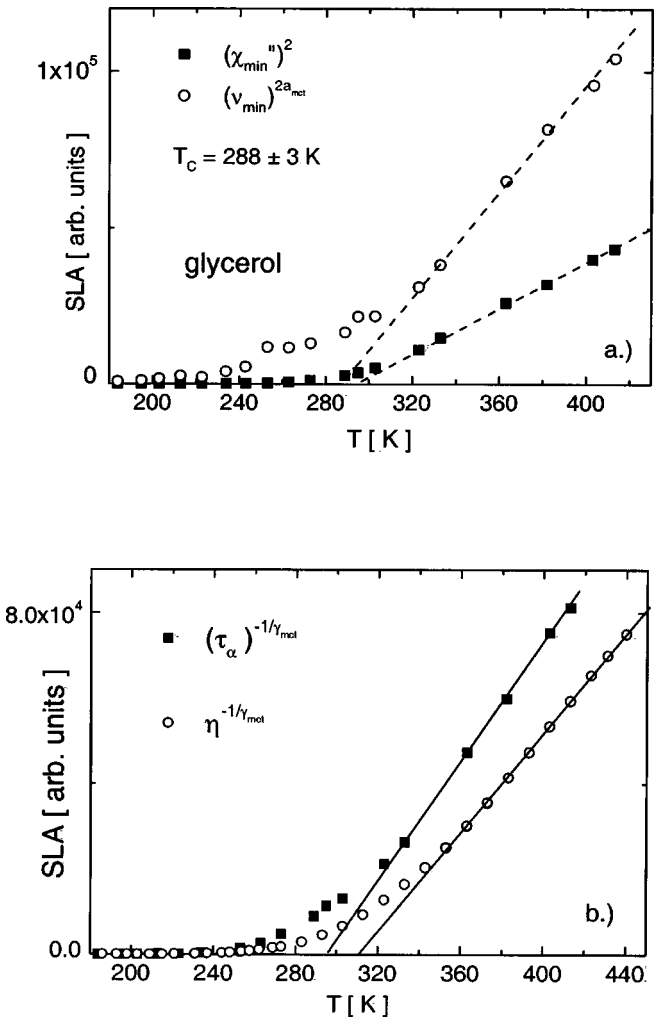

FIG. 6. (a) and (b) Testing the scaling laws of MCT, Eq. (2); the linearized scaling law amplitudes (SLA) are plotted; in (a) the two points at highest temperatures were obtained from the master curve in Fig. 7.

Finally, having achieved a complete interpolation of the susceptibility data we can proceed to checking another MCT prediction, namely, the anomaly of the nonergodicity parameter f, by applying Eq. (11). For the cutoff frequency we introduce $\nu_c = 200$ GHz, which ensures that essentially no spectral contribution of the boson peak is included in the integral. Of course, this limit is somewhat arbitrary, but a change from $\nu_c = 200$ to $\nu_c = 400$ GHz leads to an increase of $1-f$ by a factor of roughly 2^a, i.e., only 23% at high temperatures (as $a \cong 0.3$). Figure 8 displays $1-f$ as a function of temperature. Below about 300 K a significant drop of $1-f$ is observed. This is nothing else than the expected anomaly, and the data in Fig. 8 can be fitted with the square root behavior of MCT, Eq. (3), yielding a critical temperature $T_c \cong 300$ K, which is somewhat higher than that extracted from the scaling laws (cf. Fig. 6). We note that the absolute value of $1-f$ is quite small; the largest value found at high temperatures is $1-f \cong 0.017$.

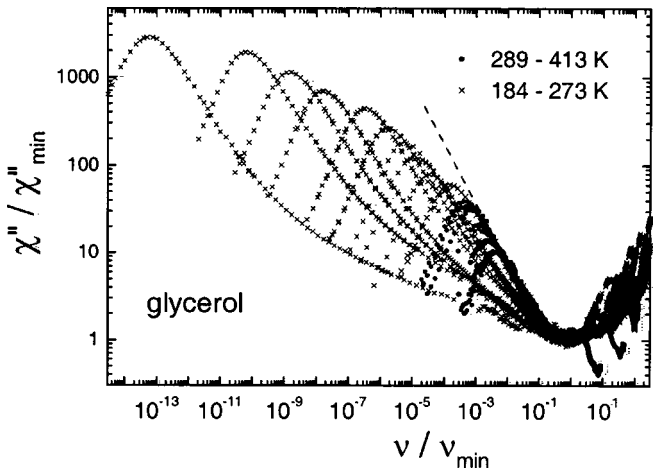

FIG. 7. Rescaled minimum of the susceptibility obtained by scaling the original data [cf. Fig. 1(b) by $\chi_{\min}$ and $\nu_{\min}$, respectively; solid circles, data above 289 K; crosses, data below 289 K; dashed line, interpolation by the MCT master curve, Eq. (1)].

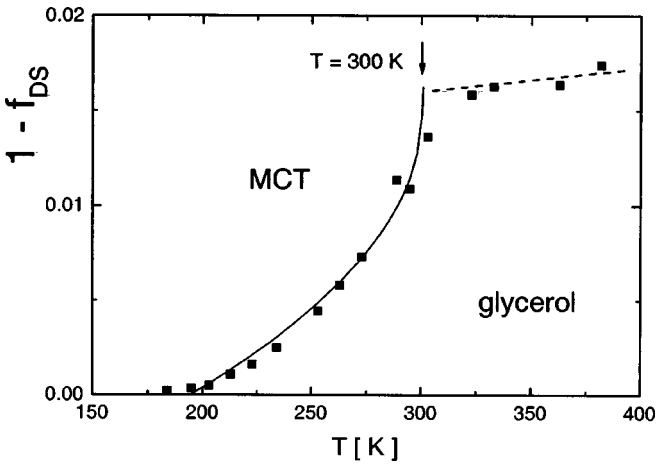

FIG. 8. Nonergodicity parameter $1-f_{\mathrm{DS}}$, cf. Eq. (11), as a function of temperature, solid line, square root law of MCT; dashed line, guide for the eye.

IV. DISCUSSION AND CONCLUSION

The evolution of the relaxational contribution in the dielectric susceptibility of glycerol has been successfully interpolated covering 17 decades in frequency. Following the lines given by Adichtchev *et al.* [5] and Blochowicz *et al.* [21], we have analyzed the low frequency response at low temperatures (including the α-process and excess wing) within a phenomenological approach, on the one hand, and the high temperature data within MCT, on the other. In the phenomenological approach the crossover temperature T_x is defined by the disappearance of the excess wing and reaching the CD limit when heating what can clearly be identified in the temperature dependence of the parameters of the applied extended generalized gamma (GGE) distribution. In the frame work of MCT the crossover is given by the result of the scaling analysis. Within the experimental error both crossover temperatures (T_x and T_c) agree, and $T_c \cong 288$ K is extracted from a MCT analysis. The present MCT analysis uses all available high temperature data ($T \leqslant 413$ K) while Lunkenheimer *et al.* restricted their analysis to temperatures $T \leqslant 333$ K [17]. Also, dielectric spectra normalized by the static permittivity are analyzed. As a consequence of both, the critical temperature extracted shifted to higher temperatures by roughly 30 K as compared to 262 K in the previous analysis, and consistent results are achieved from all scaling observables. As in the case of toluene [4] and picoline [5], for reasons not completely understood, the asymptotic laws of MCT describe the dynamics even up to highest temperatures also in the case of glycerol. Only by including that data, a safe foundation for extracting the critical temperature is guaranteed. This is particularly crucial for nonfragile organic glass formers for which the high temperature scenario of MCT may be observed only well above the room temperature. Thus, it may be possible that discrepancies in determining T_c found also for other systems disappear when the MCT analysis is extended to highest temperatures including even temperatures above the melting point. We note that reinspecting the data of the neutron scattering study of glycerol suggests $T_c \cong 280$ K [6] and that Rössler *et al.* reported $T_c \cong 300$ K from an analysis of the viscosity [15]. Applying the so-called Stickel plot, Lunkenheimer *et al.* [17] found that the Vogel-Fulcher-Tammann equation holds well only below 285 K.

In addition to extracting T_c from the scaling analysis, T_c can equally well be identified by the anomaly of the nonergodicity parameter f, respectively, $1-f$. Evaluating the corresponding integrals over the susceptibility by using the fit curves obtained within the phenomenological approach, $1-f(T)$ is easily determined. In good agreement the square root behavior of MCT is rediscovered. The absolute value of $1-f$ is very small, i.e., $1-f \leqslant 0.02$ is observed. Thus, experimentally, it does not make much sense in most cases to determine the anomaly by extracting $f(T)$ since the latter is close to 1. This may have important consequences since small values of $1-f(T)$ may also show up in an analysis of depolarized LS spectra [1]. Assuming in first approximation that LS describes the reorientational correlation function of the second Legendre polynomial and dielectric spectroscopy the corresponding function of the first Legendre polynomial and the fast motion can be described by a spatially highly restricted reorientation within, e.g., a cone model, Blochowicz *et al.* showed that $1-f_{\mathrm{LS}} \cong 3(1-f_{\mathrm{DS}})$ [31] (cf. also Ref. [30] for a similar discussion). Thus, even for LS experiments it might be difficult to identify the anomaly of the nonergodicity parameter in $f_{\mathrm{LS}}(T)$. In the case of NS, $1-f$ may become larger [1,6]. Within molecular mode coupling theory $1-f_c(q=0) \cong 0.02$ has been reported, which is very close to the value observed experimentally [32]. In the corresponding simulations it is indeed found that $1-f_{\mathrm{LS}} > 3(1-f_{\mathrm{DS}})$ [33].

Concerning the evolution of the susceptibility, our analysis clearly discriminates between a high temperature regime and a low temperature regime. The first is well described by MCT with an α-process and fast dynamics contribution being essentially unchanged in spectral shape and amplitude and only τ_α changing, whereas the second, the low temperature scenario, is characterized by the emergence of the excess wing. The appearance of the excess wing marks the sole

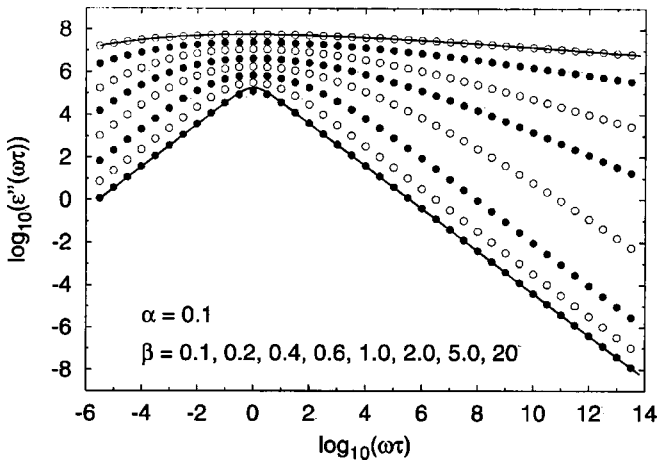

FIG. 9. Susceptibility modeled by the GGE distribution setting $\sigma=0$, i.e., no excess wing is present; the parameter α is low but constant and β is varied; curves shifted vertically for clarity. The curves can be interpolated by a KWW susceptibility (solid line).

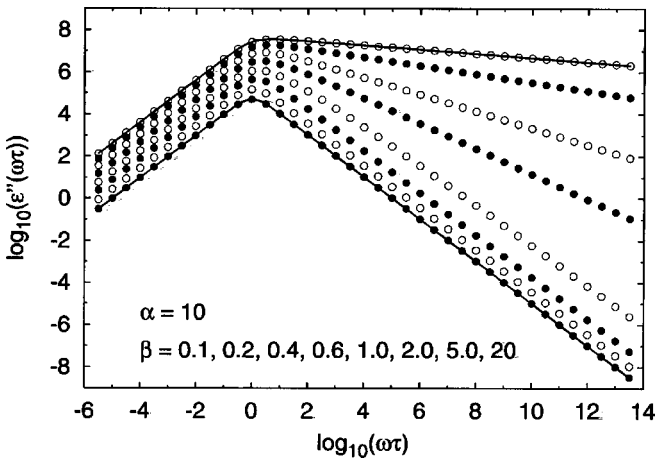

FIG. 10. Susceptibility modeled by the GGE distribution setting $\sigma=0$; the parameter α is high but constant and β is varied; curves shifted vertically for clarity. The curves can be interpolated by a Cole-Davidson susceptibility (solid line)

change of the dynamic susceptibility while cooling a type-*A* glass former and also marks the breakdown of the high temperature scenario of MCT. However, concerning the anomaly of the nonergodicity parameter $1-f$, this MCT feature is observed below T_c, thus indicating that at least this MCT prediction remains valid also at $T<T_c$. Also, below T_c the exponent a of the fast dynamics contribution shows a trend to increase, which tentatively may be interpreted as a crossover to a white noise spectrum [5,6]—a feature also predicted by MCT though only at frequencies below the ''knee,'' which actually is not found.

Comparing different glass formers such as glycerol, propylene carbonate, and 2-picoline, it appears that the crossover is always found in the range $10^{-9}<\tau_\alpha<10^{-8}$ s. In the case of glycerol $\tau_\alpha(T_c)\cong 2\times 10^{-9}$ s is observed, and the critical temperature $T_c=288$ K is actually very close to the melting point $T_m=290$ K. In other words, in the nonfragile glass former glycerol the dynamics slows sufficiently down already above the melting point. Thus, one may say that it is not the degree of supercooling but rather a sufficiently high viscosity that marks the dynamic crossover.

As discussed the excess wing is hardly to be taken as a part of a continuing ($T<T_c$) α-process but rather as a special secondary relaxation process [22,23]. This process manifests itself in a very similar way in all type-*A* glass formers when the line-shape parameters are plotted as functions of the time constant τ_α. No significant difference is found between the fragile system propylene carbonate and glycerol exhibiting an intermediate degree of fragility and both systems follow the MCT predictions at high temperatures. The only important difference found for the spectral shape of the susceptibility refers to the shape of the α-relaxation peak itself. The width parameter α is temperature independent but different for the various systems. In other words, only the slowest dynamics exhibit nonuniversal features. Future experiments on other type-*A* glass formers, which essentially have to cover all experimentally accessible frequencies, will reveal whether this statement survives progress. First analysis of type-*B* glass formers indicates that some universality is lost (depending on the relaxation strength of the β-process) but still both the excess wing as well as the β-process contribution itself happen to merge with the α-process at the critical temperature [21]. Concluding, we say that although clarifying the physical nature of the slow response of a glass former with an emergence of the excess wing is still a future task to be solved, the proposed approach yields a complete interpolation of the susceptibility spectra of type-*A* glass formers, provides a clear cut identification of the spectral changes occurring while supercooling, and reproduces the MCT scenario at high temperatures, i.e., allows for determining unambiguously the critical temperature T_c also in the case of nonfragile systems.

ACKNOWLEDGMENTS

We thank P. Lunkenheimer for providing us with the permittivity data of glycerol and also for clarifying discussions and A. Brodin for critically reading the manuscript. The advice of R. Schilling is appreciated.

APPENDIX

The GGE distribution applied in the present contribution describes the shape of the α-relaxation peak by two parameters, namely, α and β, and the excess wing by σ and γ. The significance of the latter parameters is straightforward: Parameter σ is a measure of the onset of the excess wing (with respect to τ_α) and parameter γ represents the corresponding power-law exponent. In the case of parameters α and β, the situation is less obvious, and in what follows we want to demonstrate its respective role. We note that a detailed discussion of the GGE function is also found in Ref. [21]. In order to concentrate on describing the α-relaxation peak itself we set $\sigma=0$, thus, a distribution without excess wing contribution is considered. In this case the GGE distribution transforms into a generalized gamma distribution (GG) [21], and the role of parameters α and β can easily be singled out.

In Fig. 9 the susceptibility applying the GG distribution is

plotted for a constant but low parameter $\alpha=0.1$ and varying β values. For all curves, β fixes the limiting high frequency power law provided that $\beta\leqslant 1$, for $\beta>1$ the corresponding power-law exponent is always 1 and the susceptibility becomes close to a Debye curve. In the limit $\beta\rightarrow\infty$ the GG distribution becomes a δ function. In Fig. 10 we display the susceptibility for a constant but high $\alpha=20$ and varying β values. Again β fixes the power-law exponent for $\beta\leqslant 1$. The difference of the two sets of curves is given by the change of the susceptibility at frequencies lower than the maximum frequency when β is systematically increased. Whereas in Fig. 10 the low frequency power law extends essentially up to susceptibility peak, this is not the case in Fig. 9. In the latter case the crossover from the low frequency power law to the peak sets in a much lower frequencies, and these curves may be interpolated by a Kchlrausch-Williams-Watts (KWW) function (solid lines), whereas in Fig. 10 the curves are rather fitted by a Cole-Davidson susceptibility (solid line). In other words, a low α allows an increasing β parameter to produce a KWW character whereas with a high α, a CD type of susceptibility is reproduced.

Of course, both parameters α and β may be somehow correlated in a fitting procedure. Also we note that the power law defined by parameter β is actually not seen if an excess wing is present, but still β fixes the width of the α-peak. As mentioned in the text, a reliable estimate of α is found if a free fit with the GGE distribution is performed for a dataset close to T_g. Here, the excess wing is most pronounced and separate from the α-relaxation peak. It turned out that fixing α in this way, it can be kept constant for all temperatures, and the particular value of α distinguishes the different glass formers. As the effect of α on the manifestation of the α-relaxation peak saturates at high values of α it may be advisable to take rather $1/\alpha$ as a convenient width parameter.

[1] P. Lunkenheimer, U. Schneider, R. Brand, and A. Loidl, Contemp. Phys. **41**, 15 (2000).
[2] G. Li, W. M. Du, A. Sakai, and H. Z. Cummins, Phys. Rev. A **46**, 3343 (1992).
[3] H. Z. Cummins, G. Li, W. M. Du, J. Hernandez, and N. J. Tao, Transp. Theory Stat. Phys. **24**, 981 (1995).
[4] J. Wiedersich, N. Surovtsev, and E. Rössler, J. Chem. Phys. **113**, 1143 (2000).
[5] S. Adichtchev, St. Benkhof, T. Blochowicz, V. Novikov, E. Rössler, and J. Wiedersich, Phys. Rev. Lett. **88**, 055703 (2002).
[6] W. Petry and J. Wuttke, Transp. Theory Stat. Phys. **24**, 1075 (1995).
[7] A. Tölle, Rep. Prog. Phys. **64**, 1473 (2001).
[8] W. Kob and H. C. Anderson, Phys. Rev. E **51**, 4626 (1995).
[9] W. Götze and L. Sjögren, Rep. Prog. Phys. **55**, 241 (1992).
[10] W. Götze, J. Phys.: Condens. Matter **11**, A1 (1999).
[11] L. M. Torrel, L. Borjesson, and A. P. Sokolov, Transp. Theory Stat. Phys. **24**, 1097 (1995).
[12] E. Rössler and A. P. Sokolov, Chem. Geol. **128**, 143 (1996).
[13] B. Ruffĺe, S. Beaufils, B. Toudic, C. Ecolivet, A. Le Sauce, and R. Marchand, J. Non-Cryst. Solids **235-237**, 244 (1998).
[14] J. Wuttke, J. Hernadez, G. Coddens, H. Z. Cummins, F. Fujara, W. Petry, and H. Sillescu, Phys. Rev. Lett. **72**, 3052 (1994).
[15] E. Rössler, A. P. Sokolov, A. Kisliuk, and D. Quitmann, Phys. Rev. B **49**, 14 967 (1994).
[16] T. Franosch, W. Götze, M. R. Mayr, and A. P. Singh, Phys. Rev. E **55**, 3183 (1997).
[17] P. Lunkenheimer, A. Pimenov, M. Dressel, Yu. G. Goncharov, R. Böhmer, and A. Loidl, Phys. Rev. Lett. **77**, 318 (1996).
[18] D. M. Paolucci and K. A. Nelson, J. Chem. Phys. **112**, 6725 (2000).
[19] D. Prevosto, P. Bartolini, R. Torre, M. Ricci, A. Taschin, S. Cappacioli, M. Lucchesi, and P. Rolla, Phys. Rev. E **66**, 011502 (2002).
[20] A. Kudlik, S. Benkhof, T. Blochowicz, C. Tschirwitz, and E. Rössler, J. Mol. Struct. **479**, 201 (1999). We note that due to an error appearing after proofreading the formula of the GGE distribution is presented incorrectly.
[21] T. Blochowicz, C. Tschirwitz, St. Benkhof, and E. A. Rössler, J. Chem. Phys. **118**, 7544 (2003).
[22] U. Schneider, R. Brand, P. Lunkenheimer, and A. Loidl, Phys. Rev. Lett. **84**, 5560 (2000).
[23] M. Vogel, C. Tschirwitz, G. Schneider, C. Koplin, P. Medick, and E. Rössler, J. Non-Cryst. Solids **307-310**, 326 (2002).
[24] F. Mezei and M. Russina, J. Phys.: Condens. Matter **11**, A341 (1999).
[25] T. Nicolai, J. C. Gimel, and R. Johnson, J. Phys. II **6**, 697 (1996).
[26] C. J. F. Böttcher and P. Bordewijk, *Theory of Electric Polarization* (Elsevier, Amsterdam, 1996), Vol. II.
[27] P. Lunkenheimer, Habilitationsarbeit, Augsburg, 2000.
[28] A. Schönhals, Europhys. Lett. **56**, 815 (2001).
[29] Landolt-Börnstein, II. Band, Teil 5, Bandteil a (Transportphänomene I), Berlin, 1969.
[30] M. J. Lebon, C. Dreyfus, Y. Guissan, R. M. Pick, and H. Z. Cummins, Z. Phys. B: Condens. Matter **103**, 433 (1997).
[31] T. Blochowicz, A. Kudlik, S. Benkhof, J. Senker, E. Rössler, and G. Hinze, J. Chem. Phys. **110**, 12011 (1999).
[32] R. Schilling and T. Scheidsteger, Phys. Rev. E **56**, 2932 (1997).
[33] S. Kämmerer, W. Kob, and R. Schilling, Phys. Rev. E **58**, 2141 (1998).